Chin. J. Chem. Eng., **15**(3) 345—352 (2007)

Numerical Simulation of Separating Gas Mixtures *via* Hydrate Formation in Bubble Column*

LUO Yantuo(罗艳托)[a,b], **ZHU Jianhua**(朱建华)[a,**] **and CHEN Guangjin**(陈光进)[a]
[a] Faculty of Chemical Science & Engineering, China University of Petroleum, Beijing 102249, China
[b] PetroChina Planning & Engineering Institute, Beijing 100083, China

Abstract To develop a new technique for separating gas mixtures *via* hydrate formation, a set of medium-sized experimental bubble column reactor equipment was constructed. On the basis of the structure parameters of the experimental bubble column reactor, assuming that the liquid phase was in the axial dispersion regime and the gas phase was in the plug flow regime, in the presence of hydrate promoter tetrahydrofuran (THF), the rate of hydrogen enrichment for CH_4+H_2 gas mixtures at different operational conditions (such as temperature, pressure, concentration of gas components, gas flow rate, liquid flow rate) were simulated. The heat product of the hydrate reaction and its axial distribution under different operational conditions were also calculated. The results would be helpful not only to setting and optimizing operation conditions and design of multi-refrigeration equipment, but also to hydrate separation technique industrialization.
Keywords hydrate, kinetics, separation, bubble column, numerical simulation

1 INTRODUCTION

When a gas mixture forms a hydrate, the relative concentration of each component in the hydrate phase and that in the residual vapor phase might be different. The component that can form a hydrate or form a hydrate more easily might be enriched in the hydrate phase. On the basis of this principle, a new technology of separating gas mixture through hydrate formation/decomposition was proposed, which might be applicable in economically recovering valuable gas components such as hydrogen and ethylene from refinery gases. There have been some studies reported related to the separation technology based on hydrate principles[1—8].

As the process of separating a gas mixture is usually carried out in a column reactor, a set of medium-sized experimental column reactor equipment for studying gas mixture separation *via* hydrate formation was constructed. Using the orifice bubbling gas method, in the presence of the hydrate promoter tetrahydrofuran (THF), the rate of hydrogen enrichment for CH_4+H_2 gas mixtures at different operational conditions was simulated, and some feasible operational conditions were proposed according to the simulation results. The heat product of the hydrate reaction and its axial distributing along the height of column at different operational conditions were also calculated.

2 NUMERICAL MODEL AND SIMULATION METHOD

2.1 Experimental apparatus

A brief introduction about the experimental apparatus used in this study is given here. The apparatus consists mainly of a cylindrical bubble column with sieve plates in it, a hydrate decomposer system, a gas compressor, a liquid feed pump and several heat exchange components. Flow chart of the experimental apparatus is shown in Fig.1.

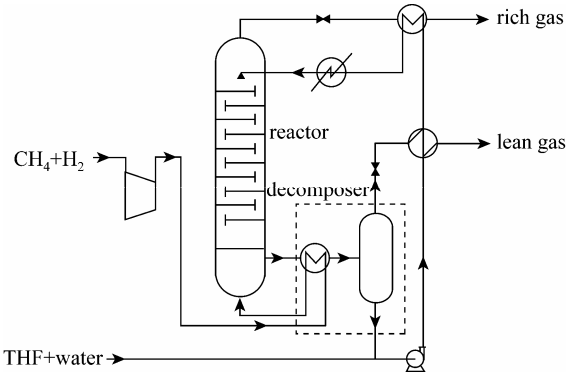

Figure 1 Experimental apparatus

Structure parameters of the experimental bubble column are shown in Table 1. Structure parameters of sieve plates are similar to that of the gas distributing implement except its area.

Table 1 Parameter values of the experimental apparatus

Parameters	Values
H_t, m	7.0
d_t, m	0.2
ΔL, m	1.0
δ, mm	10
sieve plate	
N	6
d_0, mm	1.5
l, mm	20
n	50

Received 2006-05-23, accepted 2006-12-11.
* Supported by the National Natural Science Foundation of China (No.20490207).
** To whom correspondence should be addressed. E-mail: rdcas@bjpeu.edu.cn

2.2 Experimental system and conditions of simulation

Experimental system: CH_4+H_2 constitute the gas mixture feed, THF aqueous solution (5.6%, by mol) constitutes liquid feed. Methane gas forms a structure Ⅱ hydrate and from which hydrogen gas can be recovered. As the pressure of methane hydrate formation in pure water is relatively high, for example, it is 2.603MPa at 273.15K, and the induction period is relatively long, hydrate promoter THF was added into the water to lower the formation pressure, shorten the induction time, and accelerate the formation rate. THF itself can play a role in forming the structure Ⅱ hydrate in which the THF molecules occupy only the larger cavities. The number ratio of large cavities to little cavities to water molecules in the structure Ⅱ hydrate appears to be 1∶2∶17 under full occupancy[9]. When the promoter THF was added to water and made 5.6% (by mol) THF aqueous solution, it just is the molar ratio of THF to H_2O (1∶17) in hydrate that formed by THF molecules with water molecules, and the larger guest molecule THF almost exclusively occupies the large cavities, thus restricting CH_4 to only small cavities in the hydrate[10].

Experimental conditions of simulation are shown in Table 2.

Table 2 Experimental conditions of simulation

Experimental conditions	Ranges
T, K	278.15—282.15
$p\times10^{-6}$, Pa	2—6
H, m	6.0
σ, mN·m^{-1}	37.39—38.49
μ, mPa·s	2.48—134.48
U_L, m·s^{-1}	0.00116—0.0035
U_g, m·s^{-1}	0.005—0.045

2.3 Numerical model

2.3.1 *Hydrodynamic model*

Assuming that the liquid phase is in axial dispersion regime and gas phase is in plug flow regime. The axial dispersion model and plug flow model can be mathematically described as follows:

$$\frac{E}{U_L H}\frac{d^2X}{dZ^2}+\frac{dX}{dZ}+\frac{H\varepsilon_{Lh}}{U_L C_{L0}}r=0 \tag{1}$$

$$\frac{dY}{dZ}+\frac{HS\varepsilon_{Lh}}{n_0}r=0 \tag{2}$$

where E is dispersion coefficient of dispersion number $E/(U_LH)$ representing liquid back-mixing degree, and it can be calculated by Eqs.(3)—(4)[11—13]; r is the reaction velocity term that can be determined by methane hydrate formation kinetic model; X, Y, Z are all dimensionless variables, X=dimensionless concentration of CH_4 in the slurry along the column height, Y=dimensionless mole flux of CH_4 gas along the column height, Z=dimensionless distance along the column height, they are expressed in Eqs.(5)—(7), respectively; where C_{L0} is concentration of CH_4 in the slurry at the bottom of the column, mol·m^{-3}, n_0 is flow rate of gas feed at the bottom of column, mol·s^{-1}, H_0 is the height of slurry along the column; H and S denote the height of the static liquid holdup and the cross section area of the column, respectively.

$$\frac{E}{E_{no}}=U_g^{0.1}\Big/\left[1+0.5\left(\frac{d_t}{\Delta l}\right)^{0.2}\right] \tag{3}$$

$$E_{no}=1.23d_t^{1.5}U_g^{0.5} \tag{4}$$

where E_{no} stands for dispersion coefficient when there is no sieve plate in the column[13].

$$C_{Lh}/C_{L0}=X \tag{5}$$

$$n_{gh}/n_0=Y \tag{6}$$

$$h/H_0=Z \tag{7}$$

Model boundary conditions:

at $Z=0$:

$$\left.\frac{dX}{dZ}\right|_{Z=0}=0 \tag{8}$$

$$Y=1$$

at $Z=1$:

$$X|_{Z=1}=X_{in}-\frac{1}{Pe_L}\left.\frac{dX}{dZ}\right|_{Z=1} \tag{9}$$

where Pe_L stands for the Peclet number of the liquid phase, and $1/Pe_L=E/(U_LH)$, X_{in} is the dimensionless concentration of CH_4 in the liquid feed and $X_{in}=0$.

2.3.2 *Hydrate formation kinetic model*

On the basis of previous experiments, the kinetic model of methane hydrate formation in the presence of a hydrate promoter THF in a bubble column was advanced[14]. In the kinetic model, the methane hydrate formation rate was expressed by CH_4 consumption rate r_{CH_4}/a (mol·min^{-1}·m^{-2}). The kinetic model was as follows:

$$r_{CH_4}/a=2k\theta_{CH_4}\left[e^{q\left(\frac{-\Delta G}{RT}\right)}-1\right] \tag{10}$$

where k and q are model parameters and k=0.50741mol·min^{-1}·m^{-2}, q=9.90464; a is the specific gas-liquid interfacial area; θ_{CH_4} represents the fraction of the small cavities occupied by CH_4 molecules; $-\Delta G/RT$ is the driving force of the hydration reaction. θ_{CH_4} and ΔG can been calculated as follows:

$$\theta_{CH_4}=\frac{cf_{CH_4}}{1+cf_{CH_4}} \tag{11}$$

$$\Delta G=\left[\lambda_2\ln\frac{f^0}{f_{THF}}+\lambda_1\ln\left(1-\theta_{CH_4}\right)\right]RT \tag{12}$$

where c is Langmuir constant; f_{CH_4} is the fugacity of

CH_4 gas; f^0 is the fugacity of the basic hydrate when $\theta_{CH_4}=0$; f_{THF} is the fugacity of tetrahydrofuran (THF); R is gas constant; λ_1 and λ_2 are structure constants of hydrate, and $\lambda_1=2/17$, $\lambda_2=1/17$, respectively. Detailed calculations of θ_{CH_4} and $-\Delta G/RT$ are shown in the literature [14].

2.4 Simulation method

Gas with liquid is a counter-current flow in the bubble column. On account of CH_4 gas continuously forming a hydrate in the course of bubbles rising, it results in the gas flux continuously decreasing from the bottom of the column to the column top. The decrease of gas flux will affect gas-liquid interfacial areas and gas resident time, and finally affect the quantity of hydrate formation. The hydrate flows downward with liquid at the same velocity because its density almost equals to liquids' and its particles are fine. Consequently the hydrate volume fraction in the slurry is increased from the column top to the column bottom. The increase of the hydrate volume fraction will affect the hydrate formation rate also.

On the basis of the reaction process mentioned above, a tiny element method to simulate the gas mixture separation process via hydrate formation is used. Divide the column into J elements along the column axis from the bottom to the top and each element is a tiny CSTR reactor, hence the whole column reactor is equal to J elements series connection.

2.4.1 *Quantity of CH_4 consumed*

The quantity of CH_4 consumed in each element can be calculated by Eq.(11):

$$n_j^{CH_4}=\int_0^t r\mathrm{d}t=r\cdot a_j\cdot t_j \tag{13}$$

where subscript j stands for no j element; r, a_j and t_j are CH_4 consumption rate, r_{CH_4}/a, gas-liquid interfacial area, and reaction time in No. j element, respectively.

The specific gas-liquid interfacial area a_j and bubble average diameter in each element can be calculated by equations that are proposed by Akita and Yoshida[15]:

$$a_j=\frac{1}{3}\left(\frac{gd_t^2\rho_L}{\sigma_L}\right)^{0.5}\left(\frac{gd_t^3}{\nu_L^2}\right)^{0.1}\frac{\varepsilon_{g,j}^{1.13}}{d_t}\cdot\left(\frac{\pi}{4}d_t^2\cdot d_j\right) \tag{14}$$

$$\frac{\varepsilon_{g,j}}{\left(1-\varepsilon_{g,j}\right)^4}=0.20\left(\frac{gd_t^2\rho_L}{\sigma_L}\right)^{1/8}\left(\frac{gd_t^3}{\nu_L^2}\right)^{1/12}\left(\frac{U_{g,j}}{\sqrt{gd_t}}\right) \tag{15}$$

$$d_j=26\left(\frac{gd_t^2\rho_L}{\sigma_L}\right)^{-0.5}\left(\frac{gd_t^3}{\nu_L^2}\right)^{-0.12}\left(\frac{U_{g,j}}{\sqrt{gd_t}}\right)^{-0.12}d_t \tag{16}$$

From Eqs.(13)—(16), you can find that the factors that influence the quantity of CH_4 consumed in each element are θ_{CH_4}, $(-\Delta G/RT)$, ν_L, a_j, t_j.

Different height of the element designed will affect gas bubble residence time and simulation results. Therefore, a reasonable height of the element should be selected. According to surface renewal theory[16], it is considered that gas bubble begins mass transfer with the liquid touching it at its top. The liquid continuously absorbs gas from the gas bubbles and forms hydrate when gliding downwards, and the liquid touching the bubble foremost has to be substituted by a new liquid element after the bubble rises a distance of the bubble diameter. Therefore, it was assumed that the height of each element equals to the bubble average diameter in it. As the liquid phase has been activated, the reaction time in each element, namely, the bubbles' residence time in each element, can be decided by the height of each element and the rising velocity of gas bubbles in it:

$$t_j=\frac{d_j}{u_{b,j}} \tag{17}$$

Because in a homogeneous bubble flow regime, the relationship of specific gas velocity with the bubble rising velocity is as follows:

$$U_g=\varepsilon_g u_b \tag{18}$$

So, the bubble residence time in each unit can be expressed as:

$$t_j=\frac{d_j\varepsilon_{g,j}}{U_{g,j}} \tag{19}$$

On the basis of the system studied, the liquid-solid medium is considered as a homogeneous phase and introduces its effective viscosity to calculate the influence of solid particles to bubbles. The relationship of the effective viscosity of the liquid-solid mixture with the hydrate volume fraction in the slurry is shown in Eq.(20):

$$\mu=\mu_0+0.44\times v_h \tag{20}$$

where μ and μ_0 stand for viscosity of the liquid-solid mixture and fresh liquid respectively, v_h is the hydrate volume fraction in the hydrate slurry[17].

2.4.2 *Heat product of hydrate reaction*

As the hydrate formation reaction is an exothermic reaction, the reaction rate will be affected by the heat produced and will be likely to cease if the heat cannot be taken away. As the quantity of hydrate formed in each element is different, the heat product in each element is different too. The heat product in each element and total heat product in the column can be calculated as follows:

$$Q_j=W_j^h q^h \tag{21}$$

$$Q=\sum_{j=1}^{N}Q_j \tag{22}$$

where Q_j, Q stands for the heat product in No. j element and total heat product in the column, respectively; W_j^h is the mass of hydrate formed in each element and calculated by Eq.(23); q^h stands for the hydrate formation heat and $q^h=230\mathrm{kJ\cdot kg^{-1}}$.

$$W_j^{\mathrm{h}} = n_j^{\mathrm{h}} \times M_j^{\mathrm{h}} \tag{23}$$

where n_j^{h}, M_j^{h} represent the mole number of the hydrate and the molecular weight of the hydrate formed in No. j element, respectively, and can calculated by Eqs.(24) and (25), respectively.

$$n_j^{\mathrm{h}} = n_j^{\mathrm{CH_4}} \Big/ \left(16\theta_j^{\mathrm{CH_4}}\right) \tag{24}$$

where $\theta^{\mathrm{CH_4}}$ represents the fraction of small cavities occupied by CH_4 molecules in the hydrate, namely $\theta_{\mathrm{CH_4}}$ as mentioned above and a detailed calculations are shown in Ref.[14,18,19].

$$M_j^{\mathrm{h}} = 16M_{\mathrm{CH_4}}\theta_j^{\mathrm{CH_4}} + 8M_{\mathrm{THF}}\theta_j^{\mathrm{THF}} + 136M_{\mathrm{H_2O}} \tag{25}$$

where $M_{\mathrm{CH_4}}$, M_{THF}, and $M_{\mathrm{H_2O}}$ denote the molecular weight of CH_4, THF, and H_2O respectively; θ_j^{THF} represents the fraction of the large cavities occupied by the THF molecules and $\theta_j^{\mathrm{THF}} = 1$ for the experimental system in this study.

3 SIMULATION RESULTS AND ANALYSIS

3.1 Factors influence quantity of CH_4 consumed

As the separation result and heat product of the bubble column are decided by the quantity of CH_4 consumed, to easily explain the separation result and heat product under different experimental conditions, the changes of CH_4 consumed rate were simulated, as also the changes of its factors [$\theta_{\mathrm{CH_4}}$, $(-\Delta G/RT)$, v_{h}, a_j, t_j], along the height of the bubble column under the conditions of T = 278.15K—282.15K, p = 5MPa, U_{g}=0.01m·s^{-1}, U_{L}=0.003m·s^{-1}, y_0=0.2 (the initial fraction of CH_4 in CH_4+H_2 mixture), and the results are shown in Figs.2—7.

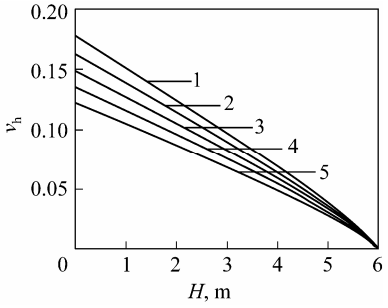

Figure 2 Changes of hydrate fraction v_{h}
(p=5.0MPa; U_{g}=0.01m·s^{-1}; U_{L}=0.003m·s^{-1}; y_0=0.2)
T, K: 1—278.15; 2—279.15; 3—280.15; 4—281.15; 5—282.15

3.2 Separation results and discussion

3.2.1 *Effect of temperature on separation process*

To research the effect of temperature on the separation process, the changes of H_2 concentration along the column height at different temperatures were calculated, and the results are shown in Fig.8.

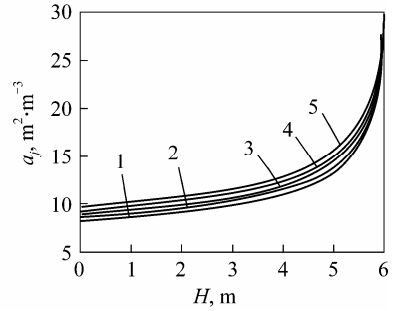

Figure 3 Changes of gas-liquid interfacial areas a_j
(p=5.0MPa; U_{g}=0.01m·s^{-1}; U_{L}=0.003m·s^{-1}; y_0=0.2)
T, K: 1—278.15; 2—279.15; 3—280.15; 4—281.15; 5—282.15

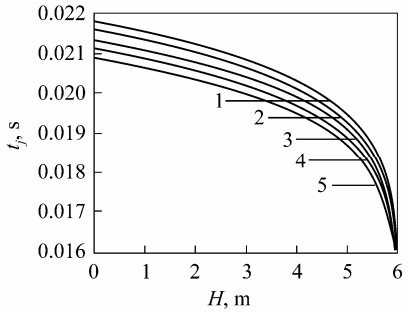

Figure 4 Changes of residence time of gas bubble t_j
(p=5.0MPa; U_{g}=0.01m·s^{-1}; U_{L}=0.003m·s^{-1}; y_0=0.2)
T, K: 1—278.15; 2—279.15; 3—280.15; 4—281.15; 5—282.15

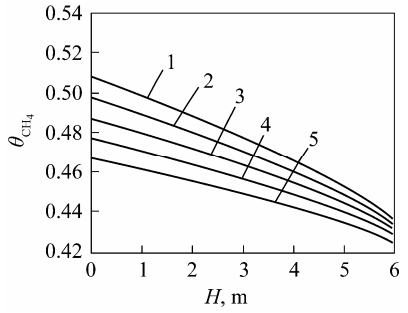

Figure 5 Changes of $\theta_{\mathrm{CH_4}}$
(p=5.0MPa; U_{g}=0.01m·s^{-1}; U_{L}=0.003m·s^{-1}; y_0=0.2)
T, K: 1—278.15; 2—279.15; 3—280.15; 4—281.15; 5—282.15

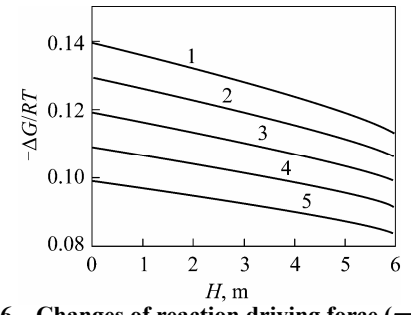

Figure 6 Changes of reaction driving force ($-\Delta G/RT$)
(p=5.0MPa; U_{g}=0.01m·s^{-1}; U_{L}=0.003m·s^{-1}; y_0=0.2)
T, K: 1—278.15; 2—279.15; 3—280.15; 4—281.15; 5—282.15

It is found that the effect of temperature on the rate of hydrogen enrichment is distinct. The lower the temperature is, the more rapid is the H_2 concentration and the higher the H_2 concentration in the final vapor phase. The main reason lies in that driving force that

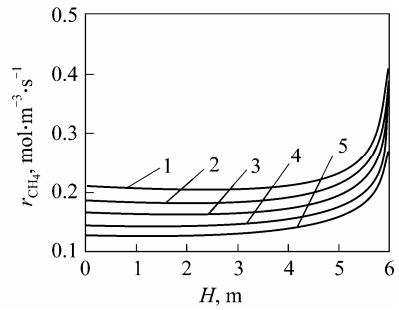

Figure 7 Changes of CH_4 consumed rate
(p=5.0MPa; U_g=0.01m·s^{-1}; U_L=0.003m·s^{-1}; y_0=0.2)
T, K: 1—278.15; 2—279.15; 3—280.15; 4—281.15; 5—282.15

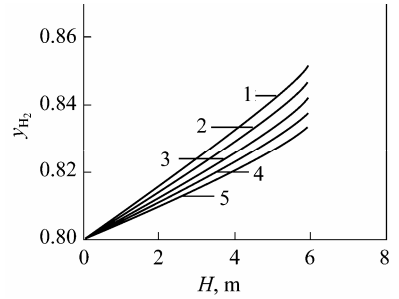

Figure 8 Effect of temperature on separation process
(p=5.0MPa; U_g=0.01m·s^{-1}; U_L=0.003m·s^{-1}; y_0=0.2)
T, K: 1—278.15; 2—279.15; 3—280.15; 4—281.15; 5—282.15

the ($-\Delta G/RT$) of the hydrate reaction increases when the temperature decreases. But the temperature cannot be too low, because THF itself can form a hydrate with water at 4.4℃ or lower temperature[20], and the bubbling separation process will not occur. So an operational temperature at about 278.15K was designed.

3.2.2 *Effect of pressure on separation process*

Effect of pressure on the separation process was also examined and the results are shown in Fig.9.

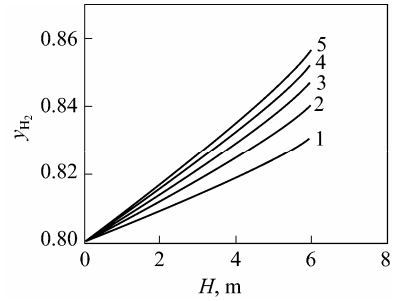

Figure 9 Effect of pressure on separation process
(T=278.15K; U_g=0.01m·s^{-1}; U_L=0.003m·s^{-1}; y_0=0.2)
p, MPa: 1—2; 2—3; 3—4; 4—5; 5—6

The simulation results show that the influence of pressure on the separation process is obvious also. The rate of hydrogen enrichment increases when pressure increases. The reason is that the fugacity difference between gas phase and hydrate phase is the driving force of the CH_4 hydrate reaction. When the temperature is constant, the higher the pressure (or the higher fugacity of CH_4 in gas phase) is, the higher the driving force is, and the higher the formation rate of CH_4 hydrate is. In addition, it can be found that the difference between the curve at p=5MPa when the curve at p=6MPa is negligible, this illustrates that an infinite increase operation pressure is meaningless in the process of gas mixture separation via hydrate formation. So, p=4MPa—5MPa as operational pressure was designed.

3.2.3 *Effect of composition of gas feed on separation process*

From Fig.10, it is found that the concentration of H_2 in the final vapor phase increases when the concentration of H_2 in the gas feed increases. But from the slopes of the curves in Fig.10, it can be seen that the rate of H_2 enrichment decreases when the concentration of H_2 in the gas feed increases. The higher the concentration of H_2 is the lower the partial pressure of CH_4 is, which causes a lower hydrate reaction driving force.

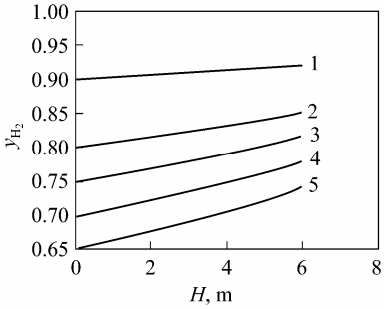

Figure 10 Effect of composition of gas feed on separation process
(T=278.15K; p=5MPa; U_g=0.01m·s^{-1}; U_L=0.003m·s^{-1})
y_0: 1—0.10; 2—0.20; 3—0.25; 4—0.30; 5—0.35

3.2.4 *Effect of superficial gas velocity on separation process*

As superficial gas velocity influences resident time and gas-liquid interfacial areas, that is to say, it influences the rate of hydrate reaction, the effect of superficial gas velocity on the separation process was studied and the simulation results are shown in Fig.11.

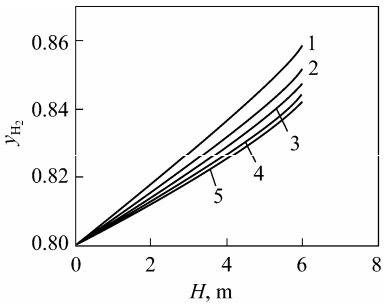

Figure 11 Effect of superficial gas velocity on separation process
(T=278.15K; p=5MPa; U_L=0.003m·s^{-1}; y_0=0.2)
U_g, m·s^{-1}: 1—0.005; 2—0.010; 3—0.015; 4—0.020; 5—0.025

The simulation results in Fig.11 show that the concentration of H_2 in the gas mixture finally achieved increases when the superficial gas velocity decreases. The reason lies in the fact that the lower superficial gas velocity causes longer resident time, and the hydrate

reaction will be more complete. But the capacity of the reactor will decrease with the superficial gas velocity reducing. So, reasonable superficial gas velocity should be chosen according to separation requirement and operational conditions.

3.2.5 *Effect of liquid flow velocity on separation process*

The liquid flow rate affects the back-mixing degree of the liquid phase and the hydrate concentration in the slurry. In other words, it influences the reaction rate. The effect of liquid flow velocity on the separation process was researched and the simulation results are shown in Fig.12.

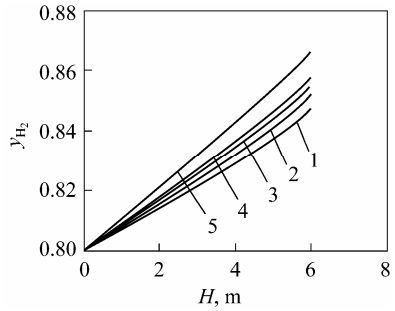

Figure 12 Effect of liquid flow velocity on separation process
(T=278.15K; p=5MPa; U_g=0.001m·s^{-1}; y_0=0.2)
U_L, m·s^{-1}: 1—0.002; 2—0.003; 3—0.004; 4—0.005; 5—0.010

It can be found from Fig.12 that the higher the liquid flow velocity is, the higher is the separation efficiency. The reason is that a higher liquid flow velocity will cause acute flow turbulence, mass transfer will be better, back-mixing will be reduced, and finally, the result in reaction rate will increase.

3.3 Reaction heat product and its axial distribution

Hydrate reaction is an exothermic reaction, and the heat product will affect the hydrate reaction rate if the heat cannot be taken away in time. So the heat product of the hydrate reaction and its axial distribution at different operational conditions were calculated.

3.3.1 *Effect of temperature on heat product and its distribution*

It is found that the effect of temperature on the heat product and its distribution is distinct. The lower the temperature is, the more the heat product is, because lower temperature is advantageous for hydrate reaction. In addition, heat distribution along the height of the column is different at different temperatures. So, the heat has to be removed based on the heat distribution curves.

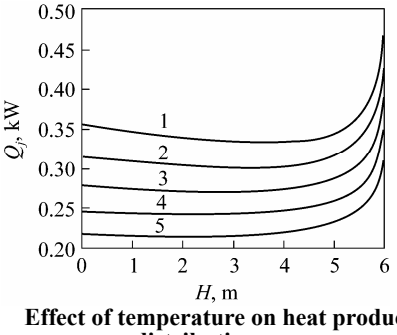

Figure 13 Effect of temperature on heat product and its distribution
(p=5MPa; U_g=0.01m·s^{-1}; U_L=0.003m·s^{-1}; y_0=0.2)
1—T=278.15K, Q=191.84kW; 2—T=279.15K, Q=177.32kW; 3—T=280.15K, Q=163.76kW; 4—T=281.15K, Q=149.82kW; 5—T=282.15K, Q=136.61kW

3.3.2 *Effect of pressure on heat product and its distribution*

As higher pressure is favorable for a hydrate reaction, the heat product increases when the operational pressure increases. From Fig.14, it is found that heat distribution along the height of column is different at different pressures. The heat distribution is even along the height of the column when p=2MPa and 3MPa, whereas, the heat distribution gradually concentrates at the central section and top of the column when p=5MPa and 6MPa.

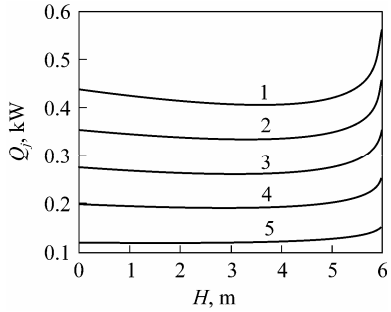

Figure 14 Effect of pressure on heat product and its distribution
(T=278.15K; U_g=0.01m·s^{-1}; U_L=0.003m·s^{-1}; y_0=0.2)
1—p=6MPa, Q=225.01kW; 2—p=5MPa, Q=191.84kW; 3—p=4MPa, Q=157.09kW; 4—p=3MPa, Q=120.75kW; 5—p=2MPa, Q=81.15kW

3.3.3 *Effect of composition of gas feed on heat product and its distribution*

The effect of gas feed composition on the heat product and its distribution are shown in Fig.15. It can be found that the heat product and its distribution are different with different compositions of gas feed. The lower the content of H_2 in the gas feed is, the more the heat product is, at the same time, the situation that heat concentrated gradually transfer from column

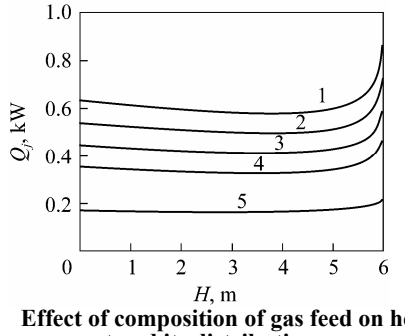

Figure 15 Effect of composition of gas feed on heat product and its distribution
(T=278.15K; p=5MPa; U_g=0.01m·s^{-1}; U_L=0.003m·s^{-1})
1—y_0=0.35, Q=301.45kW; 2—y_0=0.30, Q=266.47kW; 3—y_0=0.25, Q=229.70kW; 4—y_0=0.20, Q=191.84kW; 5—y_0=0.10, Q=107.11kW

bottom to column top. This further proves the CH_4 partial pressure's influence on hydrate reaction.

3.3.4 *Effect of superficial gas velocity on heat product and its distribution*

From Fig.16, it is clear that the total heat product increases when gas flow velocity increases. The reason is that the gas-liquid interfacial areas increase with superficial gas velocity increase, resulting in a higher reaction rate. In addition, heat distribution is significantly different under different superficial gas velocity. This is because the resident time decreases when superficial gas velocity increases, whereas the quantity of hydrate formation (or the heat product) is decided by the gas–liquid interfacial areas and gas resident time .

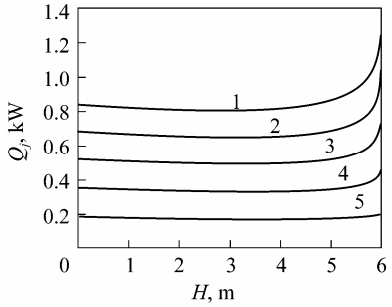

Figure 16 Effect of superficial gas velocity on heat product and its distribution
(T=278.15K; p=5MPa; U_L=0.003m·s^{-1}; y_0=0.2)
1—U_g=0.025m·s^{-1}, Q=448.25kW; 2—U_g=0.020m·s^{-1}, Q=365.22kW; 3—U_g=0.015m·s^{-1}, Q=279.87kW; 4—U_g=0.010m·s^{-1}, Q=191.84kW; 5—U_g=0.005m·s^{-1}, Q=99.92kW

3.3.5 *Effect of liquid flow velocity on heat product and its distribution*

Effect of liquid flow velocity on the heat product and its distribution are shown in Fig. 17.

As higher liquid velocity continuously brings abundant fresh liquid to the reaction system, there is better mass transfer and less liquid back-mixing finally, causing the reaction rate to increase. So it can be found in Fig.17 that the higher the liquid velocity is, the more the heat product is.

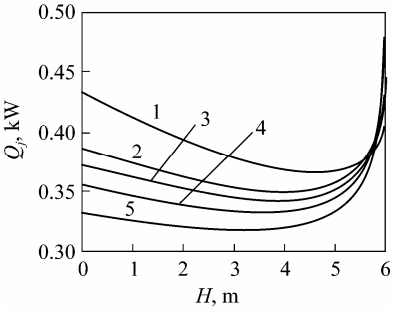

Figure 17 Effect of liquid velocity on heat product and its distribution
(T=278.15K; p=5MPa; U_g=0.01m·s^{-1}; y_0=0.2)
1—U_L=0.010m·s^{-1}, Q=260.43kW; 2—U_L=0.005m·s^{-1}, Q=219.94kW; 3—U_L=0.004m·s^{-1}, Q=207.06kW; 4—U_L=0.003m·s^{-1}, Q=191.84kW; 5—U_L=0.002m·s^{-1}, Q=171.27kW

4 CONCLUSIONS

On the basis of methane hydrate formation kinetic model, in the presence of a THF promoter in the bubble column, assuming that the liquid phase was in axial dispersion regime and the gas phase was in plug flow regime, separation efficiency of a medium-sized bubble column hydrate reactor for $CH_4 + H_2$ gas mixtures at different operational conditions was simulated. Heat product and its axial distribution along the height of the column at different operational conditions were also calculated. Some feasible operational conditions were proposed according to the simulation results, such as T=278.15K, p=4MPa—5MPa. The results of the simulation would be helpful to hydrate separation technique industrialization.

NOMENCLATURE

a	gas-liquid interfacial area, m^2·m^{-3}
C_{L0}	concentration of CH_4 in liquid at column bottom, mol·m^{-3}
d_j	height of j element, m
d_t	diameter of bubble column, m
d_0	aperture in gas distributing implement, mm
g	acceleration of gravity, kg·m·s^{-1}
H	static liquid holdup, m
H_t	height of bubble column, m
J	total number of element
ΔL	space between sieve plates, m
l	space between holes, mm
N	number of sieve plates
n	number of holes in gas distributing implement
n_0	gas flux in mole number at column bottom
p	pressure, MPa
Q	total heat product, kJ
Q_j	heat product of j element, kJ
T	temperature, K
U_g	gas flow velocity, m·s^{-1}
U_L	liquid flow velocity, m·s^{-1}
v_h	volume fraction of hydrate in slurry
y_0	mole fraction of CH_4 in gas feed
y_{H_2}	mole fraction of H_2 in gas mixture
δ	thickness of sieve plate, mm
ε_g	gas holdup
μ	viscosity of hydrate slurry, Pa·s
μ_0	viscosity of liquid, Pa·s
ν_L	kinematical viscosity of liquid, m^2·s^{-1}
ρ_L	density of liquid, kg·m^{-3}
σ_L	surface tension of liquid, N·m^{-1}

Subscripts

j	No. j tiny element

REFERENCES

1 Ballard, A.L., Sloan, E.D., "Hydrate separation processes for close-boiling compounds", In: Proceedings of the Fourth International Conference on Gas Hydrates, Yokohama, 1007—1011(2002).

2 Yamamoto, Y., Komai, T., Kawamura, T., Yoon, J.H., Kang, S.P., Okita, S., "Studies on the separation and purification of guest component", In: Proceedings of the Fourth International Conference on Gas Hydrates, Yokohama, 428—432(2002).

3 Kang, S.P., Lee, H., Lee, C.S., Sung, W.M., "Hydrate phase equilibria of the guest mixtures containing CO_2, N_2 and tetrahydofuran", *Fluid Phase Equilib.*, **185**(1/2),

101—109(2001).
4 Lee, H., Kang, S.P., "Method for separation of gas constituents employing hydrate promoter", U.S. Pat., 6602326 (2003).
5 Spencer, D.F., "Method of selectively separating CO_2 from a multicomponent gaseous stream", U.S. Pat., 6106595(2003).
6 Chen, G.J., Sun, C.Y., Ma, C.F., Guo, T.M., "A new technique for separating (hydrogen+methane) gas mixtures using hydrate technology", In: Proceeding of the 4th International Conference on Gas Hydrates, Yokohama, Japan (2002).
7 Zhang, L.W., Chen, G.J., Guo, X.Q., Sun, C.Y., Yang, L.Y., "The partition coefficients of ethane between vapor and hydrate phase for methane+ethane+water and methane+ethane+THF+water systems", *Fluid Phase Equilib*., **225**, 141—144(2004).
8 Zhang, L.W., Chen, G.J., Sun, C.Y., Fan, S.S., Ding, Y.M., Wang, X.L., Yang, L.Y., "The partition coefficients of ethylene between hydrate and vapor for methane+ethylene+water and methane+ethylene+SDS+water systems", *Chem*. *Eng*. *Sci*., **60**, 5356—5362(2005).
9 Seo, Y.T., Kang, S.P., Lee, H., "Experimental determination and thermodynamic modeling of methane and nitrogen hydrates in the presence of THF, propylene oxide, 1,4-dioxane and acetone", *Fluid Phase Equilib*., **189**, 99—110(2001).
10 Subramanian, S., Sloan, Jr. D., "Molecular measurements of methane hydrate formation", *Fluid Phase Equilib*., **158—160**, 813—820(1999).
11 Hillmer, G., Weismantel, L., Hofmann, H., "Investigations and modeling of slurry bubble columns", *Chem*. *Eng*. *Sci*., **49**(6), 837—842(1994).
12 Sekizawa, T., Kubota, H., "Liquid mixing in multistage bubble columns", *J*. *Chem*. *Eng*. *Japan*, **7**(6), 441(1974).
13 Sekizawa, T., Kubota, H., "Overall dispersion coefficient in a multistage bubble column", *J*. *Chem*. *Eng*. *Japan*, **8**(6), 507(1975).
14 Luo, Y.T., Zhu, J.H., Chen, G.J., "Experimental studies and modeling of the kinetics for methane hydrate formation with the promoter in bubble column", *J*. *Chem*. *Ind*. *Eng*. (*China*), **57**(5), 1153—1158(2006). (in Chinese)
15 Akita, K., Yoshida, F., "Bubble size, interfacial area, and liquid phase mass transfer coefficients in bubble column", *Ind*. *Eng*. *Chem*. *Proc*. *Des*. *Dev*., **13**(1), 84—91(1974).
16 Geankoplis, C.J., Transport Process and Unit Operations, 2nd edition, Allyn and Bacon, Boston (1983).
17 Sun, C.Y., "The kinetics of hydrate formation/dissociation and related topics", Ph.D. Thesis, University of Petroleum, Beijing (2001). (in Chinese)
18 Chen, G.J., Guo, T.M., "Thermodynamic modeling of hydrate formation based on new concepts", *Fluid Phase Equilib*., **122**(1), 43—65(1996).
19 Chen, G.J., Guo, T.M., "A new approach to gas hydrate modeling", *Chem*. *Eng*. *J*., **71**(2), 145—151(1998).
20 Surya, D., Alexander, G., Allan, S.M., "THF-water hydrate crystallization: An experimental investigation", *J*. *Crystal Growth*, **204**, 525—538(1999).